Solid State Electron-Hopping Transport and Frozen Concentration Gradients in a Mixed Valent Viologen−Tetraethylene Oxide Copolymer

Roger H. Terrill,† James E. Hutchison,‡ and Royce W. Murray*

Kenan Laboratories of Chemistry, University of North Carolina, Chapel Hill, North Carolina 27599-3290

Received: August 23, 1996; In Final Form: December 14, 1996[⊗]

This paper describes electrochemistry and electron- hopping dynamics for a novel viologen-based redox polymer (*poly*-V^{2+}) formed from the copolymerization of tetraethylene glycol di-*p*-tosylate and 4,4′-bipyridine. Current−potential responses and electron-hopping (i.e., self-exchange) rates have been measured for mixed valent films of *poly*-V^{2+} on interdigitated array electrodes contacted by tetrahydrofuran/acetonitrile/tetrabutylammonium perchlorate electrolyte solution and as dry mixed valent films in vacuum or dry nitrogen. Electron transfer rates vary with the mixed valency composition of *poly*-$V^{2+/+}$ films (judging film composition from the electrolysis potential with the Nernst equation) according to bimolecular reaction theory for solvent-wetted but less well for dry films. Current−potential characteristics are also reported for mixed valent films that contain concentration gradients of the *poly*-V^{2+} and *poly*-V^{+} redox states, which we attempt to freeze into place by drying the film under a gradient-generating potential bias so as to immobilize the film's counterions. Current transients at room and reduced (−30 °C) temperature show that the room-temperature responses of films containing concentration gradients are sensitive to small changes in *poly*-$V^{2+/+}$ oxidation state at the electrode/polymer interfaces.

Electron transport by self-exchange or hopping reactions in mixed valent molecular materials, especially redox polymers, has experienced considerable recent research.[1,2] Work on design and synthesis of chemical microstructures[3] has sought to exploit[4] the rich variability of molecular and polymeric properties so as to imitate electronic and optical elements such as memory units, diodes, transistors, chemical and physical sensors, and electrochromic and nonlinear optical devices. Some of the reported microstructures[5] are based on a spatially defined change in chemical composition, as in the charge-trapped bilayer.[5a−d] Redox polymer films containing "frozen" concentration gradients of a given redox couple are another, recently introduced[6,7] spatially defined microstructure that, in serial arrangements of multiple couples,[7] exhibit diode-like behavior. Additional redox materials suitable for the generation of frozen gradient microstructures are needed for the exploration of their electrical properties.

This report describes electron transport in a new, viologen-based redox polymer under conditions where, in mixed valent form, it is a mixed conductor (solvent-wetted, both ionically and electronically conducting) and under conditions where it is solely an electronic conductor (dry, ionically poorly conductive). This combination of properties is important, respectively, in establishing and then maintaining concentration gradient microstructures. The electron transport characteristics of the mixed valent viologen are investigated in the mixed conduction and electronic conductivity regimes. The electrical properties of mixed valent films containing frozen gradients are shown to be much more sensitive to residual ionic conductivity of the dry polymeric phase than are those of mixed valent films with a uniform distribution of redox sites.

The redox polymer is the previously unreported[8] viologen copolymer **I** abbreviated here as *poly*-V^{2+}. This amber,

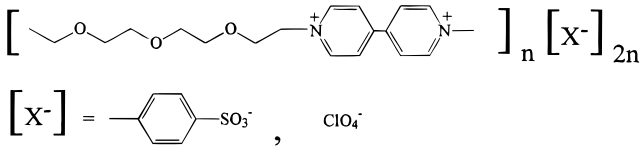

hygroscopic, copolymer is formed from the condensation polymerization of 4,4′-bipyridine and tetraethylene glycol di-*p*-tosylate. *poly*-V^{2+} is *ca.* 2 M in viologen sites, can be stably converted to the *poly*-V^{+} and (less stably[9]) *poly*-V^{0} states, is highly water and alcohol soluble, is ionically conductive when contacted by a tetrahydrofuran/acetonitrile mixture,[10] and, important to the current study, has low ionic conductivity when dry. This polymer has other attractive properties being solvent castable, fluid at *ca.* 70 °C, and adherent to electrode surfaces. The polymer is by polarized light microscopy not birefringent (crystalline) at room temperature, but produces highly oriented fibers of the polymer when drawn from its melt phase. We have previously studied[6] frozen concentration gradients in a monomeric analog of *poly*-V^{2+} that was a room-temperature molten salt. The lower ionic conductivity of *poly*-V^{2+} has allowed a more complete analysis of the behavior of films containing frozen concentration gradients. Electron transport in mixed valent forms of the viologen polymer occurs by *poly*-$V^{2+/+}$and *poly*-$V^{+/0}$ self-exchange reactions; owing to its polymeric nature, macroscopic physical diffusivity of the viologen sites is expected to be negligible.

The experiments described are as follows: (i) Electron-hopping transport by the *poly*-$V^{2+/+}$ and *poly*-$V^{+/0}$ redox couples is measured in thin films of ionically conductive, solvent-contacted *poly*-$V^{2+/+/0}$ on 2 μm gap interdigitated array (IDA) electrodes[11] (Figure 1); the observed kinetic differences between the *poly*-$V^{2+/+}$ and *poly*-$V^{+/0}$ couples are consistent with other studies.[1m,8b,12] (ii) Electronic conductivities of dry, ionically nonconductive films that are mixed valent and spatially uniform in composition (referred to as "uniform" films) were studied as a function of their *poly*-$V^{2+/+}$ concentration ratios and compared to the bimolecular reaction conduction model[1a−c,f−h,13] illustrated in Figure 1 (bottom). (iii) Finally, the current/voltage responses

† Present address: Dept. Of Chemistry, University of Illinois Urbana−Champaign, Urbana, IL 61821.

‡ Present address: Dept. of Chemistry, University of Oregon, Eugene, OR 97403-1253.

[⊗] Abstract published in *Advance ACS Abstracts,* February 1, 1997.

S1089-5647(96)02614-4 CCC: $14.00

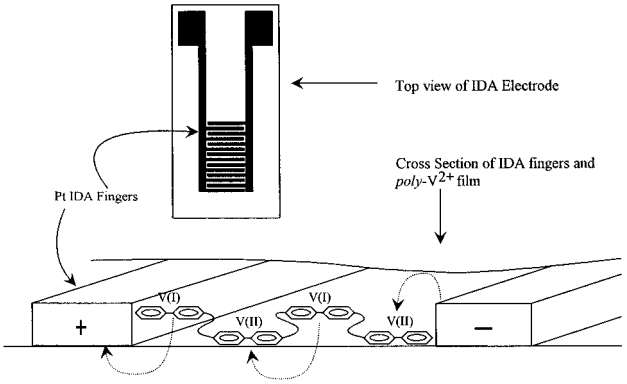

Figure 1. Schematic of an IDA electrode, showing cross section of open-face sandwich structure, and electron transfers between electrodes and *poly*-V^{2+} and *poly*-V^{+} sites (indicated by dashed arrows) in a mixed valent film in the interfinger gap under the influence of an interfinger bias.

of mixed valent *poly*-$V^{2+/+}$ films containing frozen, crossed concentration gradients (referred to as "concentration gradient" films) were studied in experiments using applied biases referenced to the original, gradient-producing potential bias. The concentration gradient in the films is prepared by electrolysis (to a steady state condition) under solvent (in an ionically conductive state) and is frozen in place by solvent removal and thorough drying to suppress ionic conductivity, while maintaining the potential bias. The $I-V$ response of films containing frozen concentration gradients is found to be (a) attenuated from that of mixed valent "uniform" sandwiches,[6] which is explained theoretically, (b) less time dependent at −30 °C than at room temperature, and (c) different for forward (same sign as the original bias) and reverse bias. The latter effects are interpreted as interfacial electrolytic changes that, owing to the low, near-interface electronic conductivity, occur in small degrees despite the low ionic conductivity of the dry polymer film.

Experimental Section

Chemicals and Synthesis of *Poly*-$V^{2+/+}$ Tosylate. Acetonitrile (Burdick and Jackson HPLC grade) and tetrahydrofuran (THF, Mallinkrodt) for electrochemical experiments were freshly distilled from CaH_2; tetrabutylammonium perchlorate (Bu_4NClO_4, Fluka Puriss electrochemical grade) was dried under vacuum at room temperature for several hours. To synthesize *poly*-V^{2+} as the tosylate salt, tetraethylene glycol di-*p*-tosylate (Aldrich 97%) and 4,4′-bipyridine (Aldrich) were mixed in CH_2Cl_2, sparged with argon (removing the solvent), and heated under Ar to 62 °C (25 min), then to 110 °C (70 min), and finally to 150 °C (1.5−2.5 h). The product material was cooled, which solidified it into a glass, and then dissolved in 70 mL of water, extracted three times with CH_2Cl_2, and reprecipitated from water into acetone. The aqueous layer was lyophilized to yield an amber, hygroscopic solid. ^{1}H NMR (D_2O): 8.84 (d, 4H, bpy), 8.21 (d, 4H, bpy), 7.37 (d, 4H, tosylate), 7.04 (d, 4H, tosylate), 4.66 (m, 4H, $-NCH_2CH_2$, partially obscured by HDO peak), 3.86 (m, 4H, $-NCH_2CH_2$), 3.45 (m, 8H, $-OCH_2CH_2O-$), 2.10 (s, 6H, tosylate methyl). No additional peaks were present. A sample, dried further overnight (50 °C, vacuum) before elemental analysis by Galbraith laboratories for C, H, and N, gave the following. Calc. for $C_{32}H_{38}N_2O_9S_2$: C, 58.34; H, 5.81; N, 4.25. Calc. for $C_{32}H_{38}N_2O_9S_2\cdot 2H_2O$: C, 55.32; H, 6.08; N, 4.03. Found: C, 55.81; H, 6.09; N, 3.94. The analyzed product was apparently a hydrate.

IDA Electrodes. Interdigitated array (IDA) electrodes consisting of 100 (n_f) interlocking 2 or 10 μm wide, 2 mm long (l) and 0.1 μm thick (h) platinum film fingers separated by 2 μm gaps and patterned on Si/SiO_2 substrates with an insulating Si_3N_4 overlayer surrounding the electrode pattern were generously donated by Nippon Telephone and Telegraph. Electrodes were cleaned by rinsing in methanol followed by a brief Ar plasma cleaning (*ca.* 16 W, 200 mT Ar flowing, 90 s) and, taking each set of IDA fingers as a working electrode, were tested using cyclic voltammetry in an aqueous $[Fe(CN)_6]^{4-}$/0.1 M KCl solution. The cyclic voltammetric currents serve to confirm the macroscopic IDA area available (the diffusion profiles from the individual fingers overlap), and the reversible 59 mV ΔE_P confirms reasonable cleanliness of the IDA fingers. The cumulative cross sectional area ($A = 9.9 \times 10^{-5}$ cm^2) of the parallel plate polymer-coated finger−gap−finger sandwiches is taken as the area of the IDA finger walls facing each other: $A = (n_f - 1)lh$.

Film Preparation. Films of *ca.* 1 μm thickness (measured by profilometry, Tencor AlphaStep 100, no surface indentation of the film was observed) were deposited from 1% methanol solutions of **I**, as the tosylate salt, onto the center of the IDA surface, using a programmed micropositioner to dispense a 2.0 μL droplet. Reproducible, round *ca.* 5 mm diameter films were obtained by dispensing the solution microdroplet and immediately withdrawing the tip as the pipet blows out residual solution. The thin films were dried in air for several minutes at room temperature, in air, and in vacuum in the electrochemical cell before exposure to electrolyte.

Conductivity and Other Measurements. The IDA was mounted in a closed cell, permitting covering the filmed IDA with liquid solvent, removing the solvent, evacuation, and N_2 backfilling without exposure to the atmosphere. For experiments in THF/CH_3CN solutions, the electrolyte solution contacted reference and auxiliary e1ectrodes as well as the IDA, permitting independent control of the IDA finger set potentials for desired electrolyses of the viologen polymer film. Dry mixed valent films were prepared by electrolysis at the desired potential (and corresponding [*poly*-V^{2+}]/[*poly*-V^{+}] ratio) for 3 min (at which time the current had decayed to baseline) followed by withdrawal of the solvent, 2 min of vigorous nitrogen purging, and 5 min of vacuum. Potential control *vs* reference electrode and interfinger bias are preserved during this process. When drying an electrolytically prepared (uniform or concentration gradient) film, in order to avoid undesirable transients, the auxiliary and reference electrodes contacted electrolyte in the filling arm of the cell in such a way that they retained continuity with one another when the working electrode compartment was dried.

Dry, mixed valent film conductivities were measured under vacuum or in flowing dry N_2 using sweeps and steps of potential bias between the IDA finger sets. The equipment for voltage sweeps and steps and for temperature control was as previously described.[6] Conductivities of mixed valent films containing frozen concentration gradient microstructures were measured using sweeps and steps that were "one-shot" cycles with potential bias returned to the bias originally used to generate the gradient (typically 0.3 V) during rest cycles.

In fitting of eq 5 (*vide infra*) to experimental $I-E$ curves, an initial estimate of the product $\rho k_{EX}'$ was made (by linear regression) from the current−potential response near zero potential (eq 3), and the parameter ρ then adjusted to optimize the overall fit to eq 5.

Results and Discussion

A brief analysis of the electron-hopping dynamics in solvent-wetted viologen polymer films and in dry, uniform mixed valent

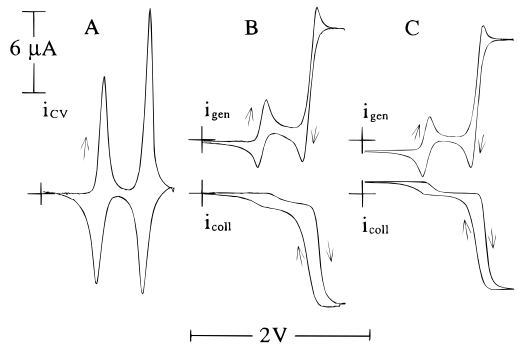

Figure 2. Room-temperature voltammetry of a *poly*-V^{2+} film on an IDA electrode with 2 μm wide fingers and 2 μm gaps, contacted by 70:30 v/v tetrahydrofuran/acetonitrile/0.1 M Bu_4NClO_4 electrolyte. Crosses are origins of current and *E vs* Ag/0.001 M Ag^+ potential axes. (Curve A) Cyclic voltammogram (3 mV/s) with IDA fingers shorted together. (Curves B) Generator and collector currents for collector−generator voltammetry with 0 V fixed potential of collector IDA fingers and 5 mV/s scan of generator IDA finger potentials. The voltammetry begins with no gradients of concentration and proceeds on the successive current plateaus to crossed concentration gradients of *poly*-$V^{2+/+}$ and of serial *poly*-$V^{2+/+}$, *poly*-$V^{+/0}$ gradients, respectively. (Curves C) Generator and collector currents for collector−generator voltammetry with −0.95 V fixed potential of collector IDA fingers and 5 mV/s scan of generator IDA finger potentials starting from 0 V. The voltammetry begins with a crossed *poly*-$V^{2+/+}$ concentration gradient and proceeds on the successive current plateaus to zero gradients (at −0.95 V generator potential) and to crossed *poly*-$V^{+/0}$ concentration gradients, respectively.

films (of *poly*-$V^{2+/+}$) was undertaken to lay the basis for analysis of hopping transport in *poly*-$V^{2+/+}$ films that contain frozen concentration gradients. The first two sections present those results.

Electron Transport in Solvent-Wetted *Poly*-$V^{2+}[ClO_4]_2$ Films. Slow potential scan (3 mV/s) cyclic voltammetry of a solvent-wetted, *ca.* 1 μm film of *poly*-$V^{2+}[ClO_4]_2$ on an IDA (with finger sets shorted together) is shown in Figure 2A. The current peaks are due to the *poly*-$V^{2+/+}$ and *poly*-$V^{+/0}$ redox couples[9] and have shapes suggestive of near-exhaustive electrolysis of the viologen film. The 520 mV separation between their formal potentials[14] is similar to that reported[8c] (500 mV) for an eight-carbon alkyl-linked viologen−polymer complexed with polystyrenesulfonic acid and contacted by aqueous electrolyte. The ΔE_{PEAK} separations between oxidation and reduction peaks likely reflect both uncompensated resistance losses within the polymer film and slowly arriving charge from electrolysis of sites within the IDA finger gaps and on the IDA periphery. The reduction peaks are consistently sharper than the corresponding oxidations. All films were potential-cycled repeatedly, which is expected to exchange the original tosylate counterions with perchlorate from the supporting electrolyte; no change in voltammetric response was evident.

In Figure 2B,C, the potentials of the IDA finger sets are independently controlled, that of one (the generator) being scanned and the other (the collector) held constant. In Figure 2B the collector is held at 0 V (the *poly*-V^{2+} state) while the generator potential is slowly (5 mV/s) scanned over the *poly*-$V^{2+/+/0}$ potential range, whereas in Figure 2C the collector is held at −0.95 V (the *poly*-V^{+} state) while the generator potential is scanned. According to the ideas of steady state electron-hopping transport developed in previous work,[1g,m,15] in Figure 2C the well-defined oxidation and reduction collector current plateaus to the left and right, respectively, of −0.95 V correspond to formation of crossed concentration gradients of the *poly*-$V^{2+/+}$and of the *poly*-$V^{+/0}$ couples, respectively. Values of the plateau collector electrode currents are related to the bimolecular electron self-exchange rate constants k_{EX} for these couples by:[1g,m]

$$i_{LIM} = \frac{10^{-3} nFAk_{EX}\delta^2 C_T^{\,2}}{6d} \qquad (1)$$

where $n = 1$, F is the Faraday constant, A (cm^2) is the contacting electrode area (see the Experimental Section), C_T is the total viologen site concentration (∼2 M, estimated from the peak charge in Figure 2A and the film volume measured by profilometry), δ (cm) and d (cm) are the viologen intersite (see footnote in Table 1) and IDA interfinger gap (2 μm) distances, respectively, the 10^{-3} factor is for conversion of dimensions, and the set of terms $k_{EX}\delta^2 C_T/6$ is the so-called electron diffusion coefficient D_E.[15] Equation 1 assumes negligible macroscopic diffusivity of the viologen sites (i.e., $D_{PHYS} = 0$). Table 1 gives values of D_E and k_{EX} (subscripted DC/DX denoting concentration gradient-based measurement) resulting from application of eq 1 to collector electrode plateau currents as in Figure 2C. These values of course represent averages over the dispersion of intersite-hopping distances and rates encountered in the mixed valent material.

Table 1 shows that the electron self-exchange rate constants $k_{EX,DC/DX}$ for the *poly*-$V^{+/0}$ couple are about 8-fold larger than those of the *poly*-$V^{2+/+}$ couple, a difference which is in good agreement with observations by others[1m,8b,12] for electron transfer dynamics in viologen polymers. The electron transfers in the present mixed valent material appear to be exceptionally facile and are, to our knowledge, larger than any yet reported[1m,16] for viologen polymers. That for the *poly*-$V^{2+/+}$couple is, however, still about 10^2-fold smaller than the corresponding k_{EX} for methyl viologen in a fluid solution.[17]

At the limiting collector electrode current at −1.7 V in Figure 2B, *poly*-V^0 is generated at the generator electrode, while the polymer at the collector electrode (0 V) is in the *poly*-V^{2+} state. In this condition the film in the IDA gap contains serial crossed concentration gradients of the *poly*-$V^{2+/+}$ and *poly*-$V^{+/0}$ couples. The agreement of this limiting current, 8.25 μA, with the 8.15 μA anticipated,[18] given the *poly*-$V^{2+/+}$ and *poly*-$V^{+/0}$ results, and the generally equal generator and collector currents mean that decomposition of *poly*-V^0 sites is not significant during the *ca.* 1 s required for an electron to transit the IDA gap (which is also the cumulative lifetime of *poly*-V^0 states generated during its transit).

Equation 1, and the analysis (*vide infra*) of frozen concentration gradient behavior *assume* that electron transport in mixed valent *poly*-$V^{2+/+}$ films occurs by bimolecular electron transfer reactions.[13] Experimental demonstrations of the reaction bimolecularity of hopping transport are not plentiful;[1a,b,e,f,13] bimolecularity means that the electron-hopping conductivity should be proportional to the *product* of the concentrations of *poly*-V^{2+} (acceptor) and *poly*-V^{+} (donor) sites in the mixed valent film. There is also the potential complication that dipositive and radical cation (1+) viologens are known to associate.[19] The electron transport was therefore examined for its reaction order.

For small potential biases, current *vs* potential is linear for hopping-based electronic conductivity of a mixed valent redox polymer and is related to the electron acceptor and donor concentrations and k_{EX} by[1a,b]

$$i = \frac{10^{-3} F^2 A\delta^2 C_D C_A k_{EX}\Delta E}{6dRT} \qquad (2)$$

where ΔE is the applied potential bias, which expressed as an

TABLE 1: Mixed Valent Viologen Electron Self-Exchange Rate Constants

	solvent-wetted films[a]		dried films[b]	
redox couple	$D_{E,DC/DX}$ (cm^2/s)	$k_{EX,DC/DX}$ (M^{-1} s^{-1})	$D_{E,DE/DX}$ (cm^2/s)	$\rho k'_{EX,DE/DX}$ (M^{-1} s^{-1})
poly-$V^{2+/+}$	$(3\pm2) \times 10^{-8}$ ($n = 13$)	$(1.1\pm0.7) \times 10^7$ ($n = 13$)	$(2\pm1) \times 10^{-8}$ ($n = 4$)	$(8\pm4) \times 10^6$ ($n = 4$)
poly-$V^{+/0}$	$(3\pm2) \times 10^{-7}$ [b]	$(9\pm6) \times 10^7$ [c]		

[a] Calculated using eq 1 from limiting currents as in Figure 2C. $\delta = [C_T N_A]^{-1/3} = 0.94$ nm, which is an approximation, treating the viologen sites as spherical. [b] $k_{EX,DE/DX}$ and $D_{E,DE/DX}$ calculated using eqs 2 and 3 from small potential bias (ohmic) regions of uniform mixed valent films. Application of eq 5 to the large potential bias current−potential responses of these films (Figure 9) produced an average value of the dispersity parameter $\rho = 8 \pm 4$. [c] These data are estimates based on observed ratios of currents for *poly*-$V^{+/0}$ and *poly*-$V^{2+/+}$ waves as in Figure 2B,C.

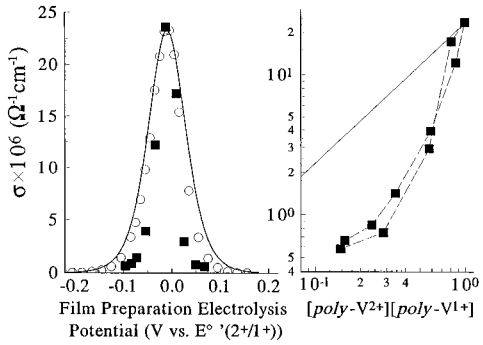

Figure 3. (Left) Redox conductivity of (○) solvent-wetted (70:30 v/v tetrahydrofuran/acetonitrile 0.1 M Bu_4NClO_4) and (■) dried (uniform mixed valent) *poly*-$V^{2+/+}$ films on 10 μm finger/2 μm gap and 2 μm finger/2 μm gap IDA electrodes, respectively, at room temperature as a function of the electrolysis potential used to prepare the mixed valent state. Solvent-wetted conductivity (○) was measured from current resulting from 10 mV bias; dried film conductivity (■) was measured from an $i-E$ trace from a ±300 mV potential sweep. Solid line is theoretical response assuming eq 3 and the Nernst equation, taking the $k_{EX} = 4.6 \times 10^6$ M^{-1} s^{-1} observed for the solvent-wetted film. The dried film conductivity data shown are normalized (divided by 3.88) to that of solvent-wetted film for this comparison. (Right) Dried film conductivity (■) replotted *vs* the calculated product [*poly*-V^{2+}][*poly*-V^+] (assuming Nernstian behavior) and the theoretical bimolecular response (solid line) assuming $k_{EX} = 4.6 \times 10^6$ M^{-1} s^{-1}.

electronic conductivity (σ) is

$$\sigma = \frac{id}{A\Delta E} = \frac{10^{-3}F^2\delta^2 C_D C_A k_{EX}}{6RT} \qquad (3)$$

Mixed valent *poly*−$V^{2+/+}$ films were prepared by electrolysis in THF/CH_3CN Bu_4NClO_4 electrolyte solution at selected potentials. The electrolysis potentials were varied by ±200 mV relative to the *poly*-$V^{2+/+}$ $E°$; at ±200 mV the predicted $C_D C_A$ product is 0.0016 M^2 (taking $C_A + C_D = 2$ M and assuming that the Nernst equation connects the electrolysis potentials to the resulting ratios, and thereby their products) of concentrations [*poly*-V^{2+}]/[*poly*-V^+] and at $E°'$ it is 1 M^2. The electronic conductivity of these films was measured at each electrolysis potential by simultaneously applying a small potential bias (10 mV) between the IDA fingers, measuring the small steady state current remaining after completion of electrolysis at each potential. The results in Figure 3 (left panel, ○, expressed as conductivity using eq 3) are compared to theory (solid line) calculated from eq 3, assuming Nernstian behavior. (This theory is equivalent to using a small bias form of eq 1.) Compared with other evaluations of bimolecularity,[1a,b,e,f,n] the correlation between the solvent-wetted experimental results (○) and theory is excellent. The agreement is least good on the outer wings of the curve, where the conductivity results suggest either that use[20] of the Nernst equation does not predict well very small values of the concentration product [*poly*-V^{2+}][*poly*-V^+] or that the mixed valent films contain some trapping or "slow" sites (such as a minor population of radical/dication dimers) whose behavior becomes more important at lowered electron fluxes.

Electron-Hopping Conductivity in Dry, Uniform Mixed Valent *Poly*-$V^{2+/+}$ Films. The small potential bias conductivity of uniform, mixed valent *poly*-$V^{2+/+}$ films prepared by electrolysis at various potentials, and then *dried*, was also examined. Electrolysis at $E°'$ ($C_D = C_A = 1$ M) is formally equivalent to the limiting current electrolysis in the solvent-wetted situation in Figure 2C and in fact gives upon application of eq 2 rate constants ($\rho k'_{EX,DE/DX}$) that agree quite well with the solvent-wetted ($k_{EX,DC/DX}$) results (Table 1). Dalton[1m] saw agreement in analogous thin electropolymerized viologen films, where the self-exchange rate constants were nearly 10^3-fold smaller than those observed in Table 1.

Experiments in which the electrolysis potential used to prepare the dried, mixed valent state of a given film was incrementally varied away from $E°'$ were greatly facilitated by the good stability of the *poly*-$V^{2+/+}$ couple and film toward repeated solvent-wetting, electrolysis, and drying. The current−potential responses of films dried for 5 min under vacuum are ohmic (at field strengths < *ca.* 10^4 V/cm). The results, shown in Figure 3 (■) and normalized at $E°'$ to conductivity of the solvent-wetted films to facilitate comparison to them and to theory, reveal (i) that electronic conductivities for the solvent-wetted and dry mixed valent films both maximize at $E°'$ as expected, but that (ii) the dry film conductivity drops off much more rapidly than ideally (Nernst equation) predicted for film compositions different from 1:1 *poly*-$V^{2+/+}$. This behavior does not necessarily represent a problem with the bimolecular rate law formulation in the solid state, as it may be an effect specific to the viologen chemical system (that is, kinetic features such as slow site traps[1b,21] or dimer formation may be more significant in the dry films and act as electron traps). These results are important to interpretation of gradient-containing-film electrical properties because those films also vary widely in composition, from *poly*-V^{2+} to *poly*-V^+ across the metal|film|metal IDA dimension.

Comparison of Uniform and Gradient-Containing, Dry *poly*-$V^{2+/+}$ Film Responses at Low Potential Bias. As mentioned earlier, a primary objective of this paper is to gain an appreciation for the electrical properties of frozen, concentration gradient-containing, mixed valent films. Such films are potential ingredients of molecular microstructures with useful electrical features.

Figure 4 shows the current−time and −potential responses of dried, non-mixed valent (only *poly*-V^{2+} states) (- - -), uniform *poly*-$V^{2+/+}$ mixed valent (—), and concentration gradient *poly*-$V^{2+/+}$ mixed valent (—•—) to 300 mV steps (left side) and ±300 mV potential sweeps (right side). Currents for the non-mixed valent film (- - -) are hardly distinguishable on these scales from zero and are much smaller than those for either mixed valent film, meaning that the ClO_4^- counterions are relatively immobile in the dried films. Currents in the mixed valent films are thus *predominantly electronic* in origin. For the uniform mixed

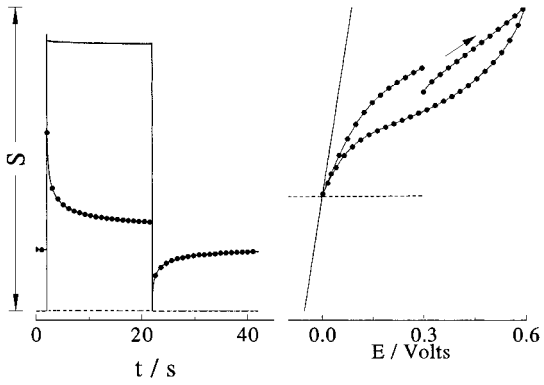

Figure 4. Current−time and current−potential responses of dried films on 2 μm finger/2 μm gap IDA electrode that are not mixed valent (*poly*-V^{2+}) **(- - -)**; uniform *poly*-$V^{2+/+}$ mixed valent (—); and mixed valent film containing *poly*-$V^{2+/+}$ crossed concentration gradient prepared by electrolysis at 300 mV interfinger bias in electrolyte (bias centered on *poly*-$V^{2+/+}$ $E^{o\prime}$) and then dried (−•−). **(**Left) Potential bias step of ΔE = 0 V to +300 mV to 0 V applied to non-mixed valent (- - -) (S = 1 μA) and uniform mixed valent (—, S = 3 μA, initial current is 0) and of ΔE = +300 mV to +600 mV to +300 mV applied to concentration gradient mixed valent film (−•−, S = 1 μA). (Right) Potential sweeps (100 mV/s) applied to non-mixed valent (- - -) (S = 1 μA) and uniform mixed valent (—) (S = 3 μA) (initial current and ΔE = 0, cross is $i-E$ origin) and to concentration gradient mixed valent film (−•−, S = 1 μA, initial current is first •, ΔE sweep is from +300 mV to +600 mV to 0V to +300 mV).

valent film (—), on a 20 s time scale, following a minor transient the currents resulting from potential steps are large and constant; those resulting from the potential sweep are quite linear with ΔE (i.e., ohmic as in eq 3) and lack any hysteresis. The absence of current transients and hysteresis in potential steps and sweeps, respectively, applied to the uniform mixed valent film further emphasizes the absence of any significant electrolytic alterations in the *poly*-V^{2+} and *poly*-V^{+} state populations at the film/finger interfaces. The ionic conductivity of the film is so much smaller than the electronic (electron-hopping) conductivity that electrolysis is unimportant on the time scale used.

The concentration gradient *poly*-$V^{2+/+}$ mixed valent (−•−) film in Figure 4, however, exhibits a long current transient in response to a potential step (left side) and substantial hysteresis upon applying a ±300 mV potential sweep (right side) centered on the initial +300 mV bias. In Figure 4, the sweep direction is, in our notation, first to forward bias (ΔE > 300 mV) and then to reverse bias (ΔE < 300 mV). The results in Figure 4 for the gradient film (−•−) have a form suggestive of electrolytic disturbances of the *poly*-V^{2+} and *poly*-V^{+} state populations (that is, the concentration gradients seem not to be truly "frozen" and the films' counterions move on the 20 s time scale). This result is in apparent contradiction to that seen for the uniform mixed valent film (—) in Figure 4; the contradiction will be rationalized below.

In a more detailed experiment (Figure 5A,B) on a *poly*-$V^{2+/+}$ concentration gradient-containing film (prepared with +300 mV bias), a series of forward (curves A, to +400, +500, +600, +700 mV) and reverse (curves B, to +200, +100, 0, −100 mV) bias potential steps were applied, in the order stated and for 20 s each, returning the potential to the original +300 mV bias for 20 s and initiating the next step in the series within the next 25 s. Figure 5C also shows the result of a potential sweep (100 mV/s) from ΔE = +300 to forward bias +900 mV and return, and from ΔE = +300 to reverse bias −300 mV and return. As in Figure 4, the currents in Figure 5 are much larger than those observed (not shown) for analogous potential steps and sweeps on a *non*-mixed valent *poly*-V^{2+} film. The Figure 5 results show (i) (curves A) long current transients for forward

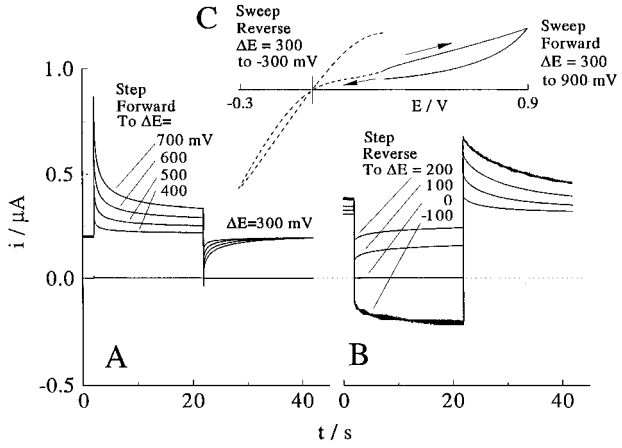

Figure 5. Dried, mixed valent film containing *poly*-$V^{2+/+}$ crossed concentration gradient on 2 μm finger/2 μm gap IDA electrode prepared by electrolysis at +300 mV bias in electrolyte solution (bias centered on *poly*-$V^{2+/+}$ $E^{o\prime}$). (Curves A) Response to forward bias potential steps from +300 mV to +400, 500, 600, 700 mV and return to 300 mV. (Curves B) Response to reverse bias potential steps from +300 mV to +200, +100, 0, −100 mV and return to 300 mV. (Curve C) 100 mV/s potential sweep, starting from +300 mV, to +900 mV forward bias (—) and then to −300 mV reverse bias (- - -).

bias steps, but shorter transients on the return step and recovery of the original current flowing at +300 mV. The forward bias currents also do not increase proportionately to the potential bias (nonohmic behavior). (ii) The current transients from reverse bias steps (curves B) have shapes that depend on the size of the bias and increase more than ohmically with ΔE, and the original currents are not quickly recovered in the return step. The sweep experiment (curve C) exhibits hysteresis and is consistent with the step results. Again, the nonohmic, hysteretic behavior seen is suggestive of electrolytic disturbance of the interfacial *poly*-V^{2+} and *poly*-V^{+} state populations, which as above was unexpected on the basis of the absence of electrolytic effects in analogous experiments (not shown) on uniform mixed valent *poly*-$V^{2+/+}$ films.

Our rationale for the observations in Figures 4 and 5 is that minute quantities of interfacial electrolysis must occur at the electrode/film *interfaces* of the *poly*-$V^{2+/+}$ concentration gradient films upon changes in the applied potential bias and that the current−potential properties of the gradient-containing films are *highly sensitive* to such changes of the interfacial *poly*-V^{2+} and *poly*-V^{+} state populations. The slow current transients resulting from potential steps are governed by time-dependent changes in the interface and near-interface resistance. Forward biasing causes an increase in interfacial resistance, and reverse biasing causes a decrease. The slow current transients cannot simply represent slow discharge of the entire stored gradient, since for example, the reverse bias step to ΔE = 0 V exhibits no current transient at all; the current immediately goes to zero, and ΔE = 0 during the sweep experiments also always yields zero current.

The preceding rationale is amplified by analysis of the spatially varying resistance expected in a gradient-containing film, which shows that *most of the resistance of a gradient-containing 2 μm thick film occurs, in fact, in the near-interface* (*ca.* 100 nm) regions. Figure 6, bottom (—) shows a resistance−distance plot calculated from eq 3 for a concentration gradient film generated with a 300 mV bias, assuming linear concentration gradients. The sharp, nearly 10^2-fold increase predicted in near-interface resistivity (relative to the center of the film) is due to the diminishing [*poly*-V^{2+}][*poly*-V^{+}] concentration product there. The near-interfacial regions also accumulate a higher *electrical* gradient relative to the center of the film; Figure

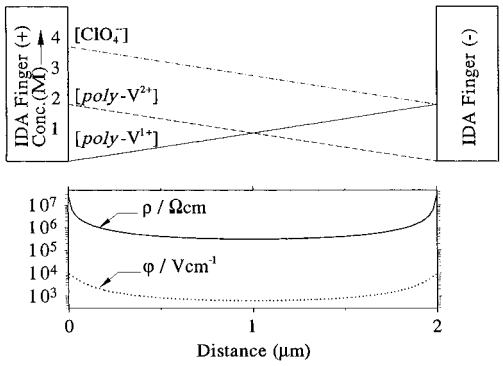

Figure 6. Schematic of crossed concentration gradient prepared at +300 mV bias on an IDA (top) and (bottom) corresponding calculated resistance (—) and electric gradient distributions (- - -) after application of +300 mV forward bias.[6]

6, bottom (···), shows the electrostatic field in a gradient film to which a forward bias of +600 mV has been applied, assuming the ions are stationary.[22] The electrical gradient is 1×10^4 and 6×10^2 V/cm at the interface and the film's center, respectively. Given the results in Figure 3, the real difference in electrical gradients is probably larger than these values. The key point is that *the large electrical gradients in the interfacial regions of gradient films can, unless the ionic mobility is extremely small, drive a small amount of counterion migration there and therefore a slow interfacial electrolysis and alteration of the interfacial poly-V^{2+} and poly-V^{+} state populations.*

In a uniform mixed valent film, the trans-film resistance is spatially equal, and thus the extant electrical gradients are uniform throughout the film and for similar applied ΔE values are also much smaller than those that develop near the interfaces (Figure 6) in a gradient-containing film. This is the reason that gradient-containing films can exhibit signs of electrolytic disturbances, while under identical conditions, uniform films do not. An important conclusion is that lack of apparent electrolytic effects in uniform mixed valent films is an insufficient criterion with which to judge that concentration gradients can be taken as adequately "frozen" in gradient-containing films. The absence of hysteresis and slow transient behavior and the presence of ohmic responses are necessary for the latter condition to be established for a gradient-containing film.

The quantity of the electrolytic disturbances in Figures 4 and 5 can be only approximately estimated. The minority states (i.e., the lower of the concentrations C_D and C_A) at the interfaces of a gradient film generated by a 300 mV bias[23] constitute only 0.3% of the interfacial sites, so a very small amount of counterion migration and consequent electrolysis could significantly change the interfacial [*poly*-V^{2+}][*poly*-V^{+}] product and the interfacial resistance. The current observed through a dried, non-mixed valent film (0.5 nA at $\Delta E = 0.3$ V), as an estimate of ionic current leading to potential electrolytic conversion, corresponds to consumption of about 5% of a monolayer[24] per second, which if distributed over a 100 nm distance would produce a 0.03% change in the minority state population over a 20 s period. These numbers suggest that the effects seen in Figures 4 and 5 correspond to electrolytic disturbances in the interfacial regions that are more than a monolayer but less than 100 nm thick.

Electrical Response of *Poly*-$V^{2+/+}$ Gradients at Lowered Temperature (−30 °C). The preceding analysis of room-temperature gradient-containing film behavior was tested by examination of films at lowered temperature. Electronic conductivity is moderately depressed by the lowered temperature (3.7×10^{-7} and 1.5×10^{-8} Ω^{-1} cm^{-1} at 25 and −30 °C, respectively). Lower temperatures typically quench ionic motions more severely than electronic hopping reactions.[6] The ionic conductivity was immeasurably small, so its change is unknown. These changes should alleviate the above parasitic ion transport and electrolysis.

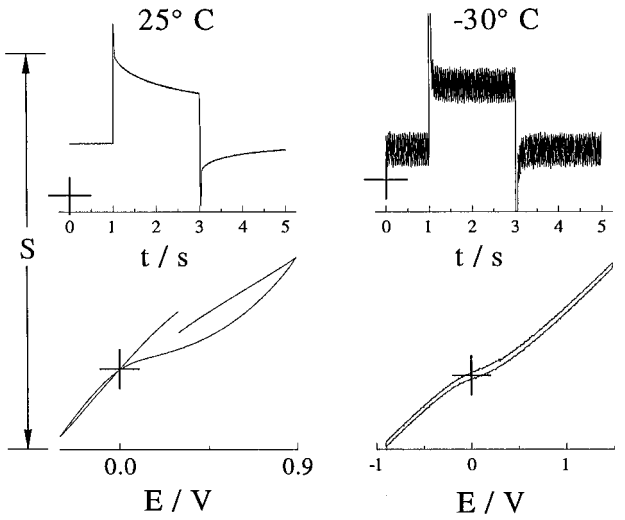

Figure 7. Response at room and at lowered temperature of a dried mixed valent film containing *poly*-$V^{2+/+}$ crossed concentration gradient (on 2 μm finger/2 μm gap IDA electrode prepared by electrolysis at +300 mV bias in electrolyte solution; bias centered on *poly*-$V^{2+/+}$ $E°'$) to forward bias potential steps (top curves) from +300 mV to +600 mV and return, and to 100 mV/s potential sweeps (bottom curves) over the indicated ranges.

Figure 7 shows results at −30 °C for a ~70 nm thick *poly*-$V^{2+/+}$ film on a 2 μm finger/2 μm gap IDA for potential steps (top) and (100 mV/s) sweeps at room temperature (left) and at −30 °C (right). In contrast to the slow current transient and current hysteresis for potential steps and sweeps seen at room temperature (Figure 7, left), the comparable low-temperature responses (Figure 7, right) exhibit, for the potential step, a brief current transient (an instrumental response) that settles to a nearly constant current, and for the potential sweep, a capacitative $i-E$ envelope lacking hysteresis. The −30 °C results are strong evidence for the absence of electrolytic disturbances upon departure from the original gradient-generating potential bias and support the above analysis of the behavior of the room-temperature *poly*-$V^{2+/+}$ concentration gradient-containing films as residing in trace electrolytic disturbances. The results also underscore the stringent ionic conductivity requirements to prepare molecular films with frozen gradients of electron-hopping transporters.

Gradient Film Electronic Conductivity as a Function of Mixed Valent Content. The relation between the electrolysis potential bias ($E_{ELECTROLYTIC}$) used to prepare a concentration gradient-containing film and its resistance can be modeled[6] if we assume that the interfacial concentrations resulting from the electrolysis are Nernstian and that the concentration gradients are linear. Then, eq 3 can be expressed as a function of distance (x) across the IDA gap and integrated to give the film resistivity R:[6]

$$R(E_{ELECTROLYTIC}) = \frac{\int_0^d \frac{dx}{\sigma(E_{ELECTROLYTIC,x})}}{d} \qquad (4)$$

Expressing the film's resistivity in this way ignores its built-in *potential* gradient and any effects attendant to this unusual situation. Figure 8 (—) plots this relation, which, as reported before, predicts decreased conductivity of gradient-containing

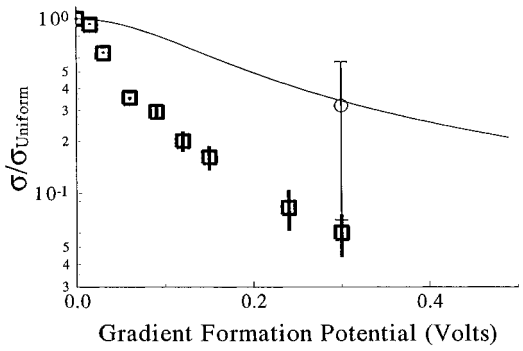

Figure 8. Relative theoretical (—) and experimental (□) conductivities of dried, uniform *poly*-$V^{2+/+}$ mixed valent films (measured with potential steps) as a function of the electrolysis potential used to prepare the mixed valent film. The electrolysis potentials applied to the IDA fingers were centered on the *poly*-$V^{2+/+}$ couple's $E^{\circ\prime}$. Vertical bars (when present) indicate the range of currents observed in a slow transient, between 20 ms and 20 s. A result from an earlier study on a related viologen melt[6] at reduced temperature (−20 to −50 °C) is also shown (○).

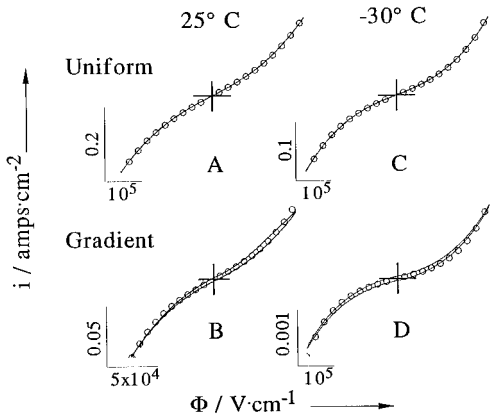

Figure 9. Comparison of current−potential response (—) of dried *poly*-$V^{2+/+}$ mixed valent films on IDA electrodes to large amplitude potential sweeps (curves A, C, D, 2 μm finger/2 μm gap, ±50 V, 50 V/s; curve B, 10 μm finger/2 μm gap, ±16 V, 400 V/s sweep). Films at the top are uniform mixed valent (50:50 *poly*-$V^{2+/+}$) and at the bottom are concentration gradient-containing (prepared by electrolysis at +300 mV bias). Temperatures are room (left) and −30 °C (right), and length of axis lines corresponds to numbers given for current and electrical gradient ϕ. Best fit to eq 5 (○) to experimental currents (—) gives (curve A) $\rho k_{EX}' = 9.5 \times 10^4$, $\rho = 3.8$; (curve B) $\rho k_{EX}' = 6.8 \times 10^4$, $\rho = 10.5$; (curve C) $\rho k_{EX}' = 3.6 \times 10^4$, $\rho = 4.1$; (curve D) $\rho k_{EX}' = 2.5 \times 10^2$, $\rho = 5.3$.

films (relative to uniform films, i.e., $E_{ELECTROLYTIC} = 0$ V), an effect mainly arising from the higher near-interfacial resistances (*vide supra*). Figure 8 also shows experimental (□) conductivities of gradient films prepared by electrolysis at +300 mV and at smaller biases. (When current transients occurred, which was only for $E_{ELECTROLYTIC} > 90$ mV, vertical bars on the symbols (□) indicate the observed range of conductivity between 20 ms and 2 s after the potential step.)

It is evident in Figure 8 that the experimental conductivities of mixed valent *poly*-$V^{2+/+}$ films containing concentration gradients fall well below those predicted by ea 4. It is likely that this discrepancy has the same (unknown) source as that in Figure 3 (■) for uniform mixed valent films.

Figure 8 also shows (open circle) a result from a previous study[6] of a similar, monomeric viologen at low temperature where the agreement with theory was better.

***Poly*-$V^{2+/+}$ Films at Large Electrical Gradients**. Figure 9A,C (—) shows the current-potential curve of a uniform *poly*-$V^{2+/+}$mixed valent film at room and at lowered temperatures. The upward curving current response is typical of an activated electron-hopping conductivity, which for *uniform* mixed valent redox films[1a,b,h,f] can be described in terms of the Marcus-based relation:

$$i = \frac{10^{-3} FA\delta C_D C_A k_{EX}'}{6}(e^{\rho F\delta\Delta E/2dRT} - e^{-\rho F\delta\Delta E/2dRT}) \quad (5)$$

where the fitting parameter ρ (ideally unity) is, as discussed in previous papers,[1a−d] added because the current−potential curves rise more steeply than classical Marcus theory predicts. The product $\rho k_{EX}'$ is equivalent to the rate constant k_{EX} of eqs 1−3, and the other symbols are as given before. The ρ appears to reflect the dispersity of electron-hopping rates in the mixed valent polymer.[1b] The fitting of eq 5 to the experimental responses is shown in Figure 9 as ○, and the kinetic results are given in the legend.

Figure 9B,D (—) shows current−potential responses from a gradient-containing *poly*-$V^{2+/+}$ mixed valent film and the theoretical fit (○) of eq 5. Equation 5 strictly does not apply to a gradient-containing film, and we show this result solely to point to the larger values that result (see figure legend) for the dispersity factor ρ. The parameter ρ is enlarged by $i-E$ curvature at large electrical gradients; in the concentration gradient-containing films the enlarged ρ (relative to uniform mixed valent films) is yet another reflection of the pileup of large electrical gradients in the resistive near-interfacial regions of gradient-containing films.

Acknowledgment. This research was supported by grants from the Department of Energy and the National Science Foundation. The authors gratefully acknowledge Osamu Niwa and Masao Morita of NTT for providing the Pt interdigitated array electrodes used in this work, and Prof. Richard P. Buck (UNC) for informative discussions.

References and Notes

(1) (a) Terrill, R. H.; Sheehan, P. E.; Long, V.; Washburn, S.; Murray, R. W. *J. Phys. Chem.* **1994**, *98*, 5127. (b) Sullivan, M. G.; Murray, R. W. *J. Phys. Chem.* **1994**, *98*, 4343. (c) Surridge, N. A.; Sosnoff, C.; Schmehl, R.; Facci, J. S.; Murray, R. W. *J. Phys. Chem.* **1994**, *98*, 917. (d) Sosnoff, C. S.; Sullivan, M. G.; Murray, R. W. *J. Phys. Chem.* **1994**, *98*, 13643. (e) Wilbourn, K.; Murray, R. W. *J. Phys. Chem.* **1993**, *92*, 3642. (f) Surridge, N. A.; Zvanut, M. E.; Keene, R. F.; Sosnoff, C. S.; Silver, M.; Murray, R. W. *J. Phys. Chem.* **1992**, *96*, 962. (g) Dalton, E. F.; Surridge, N. A.; Jernigan, J. C.; Wilbourn, K. O.; Facci, J. S.; Murray, R. W. *Chem. Phys.* **1990**, *141*, 143. (h) Jernigan, J. C.; Surridge, N. A.; Zvanut, M. E.; Silver, M.; Murray, R. W. *J. Phys. Chem.* **1989**, *93*, 4620. (i) Jernigan, J. C.; Murray, R. W. *J. Am. Chem. Soc.* **1987**, *109*, 1738. (j) Facci, J. S.; Schmehl, R. H.; Murray, R. W. *J. Am. Chem. Soc.* **1982**, *104*, 4959. (k) Chidsey, C. E. D.; Murray, R. W. *Science* **1986**, *231*, 25. (l) Han, D.; Shimada, S.; Murray, R. W.; Silver, M. *Phys. Rev. B* **1992**, *45*, 9436. (m) Dalton, E. F.; Murray, R. W. *J. Phys. Chem.* **1991**, *95*, 6383. (n) Chidsey, C. E. D.; Murray, R. W. *J. Phys. Chem.*, **1986**, *90*, 1479.

(2) (a) Rosseinsky, D. R.; Monk, P. M. S. *J. Chem. Soc., Faraday Trans.* **1994**, *90*, 1127. (b) Cannon, R. D.; Jayasooriya, U. A.; Anson, C. E.; White, R. P.; Tasset, F.; Ballou, R.; Rosseinsky, D. R. *J. Chem. Soc., Chem. Commun.* **1992**, *19*, 1445. (c) Hursthouse, M. B.; Quillin, K. C.; Rosseinsky, D. R. *J. Chem. Soc., Faraday Trans.* **1992**, *88*, 3071. (d) Rosseinsky, D. R.; Tonge, J. S. *J. Chem. Soc., Faraday Trans. 1* **1987**, *83*, 245. (e) Rosseinsky, D. R.; Tonge, J. S.; Bertheolot, J.; Cassidy, J. F. *J. Chem. Soc., Faraday Trans.* **1987**, *83*, 231. (f) Anson, F. C.; Blauch, D. N.; Saveant, J. M.; Shu, C. F. *J. Am. Chem. Soc.* **1991**, *113*, 1922. (g) Facci, J. S.; Abkowitz, M.; Linburg, W.; Knier, F. *J. Phys. Chem.* **1992**, *95*, 7908. (h) Facci, J. S.; Abkowitz, M. A.; Limburg, W. W.; Renfer, D. S.; Yanus, J. F. *Mol. Cryst. Liq. Cryst.* **1991**, *194*, 55. (i) Facci, J. S.; Stolka, M. *Philos. Mag. B* **1986**, *54*, 1. (j) Deiss, E.; Sullivan, M.; Haas, O. *J. Electroanal. Chem.* **1994**, *378*, 93. (k) Ren, X.; Pickup, P. G. *J. Electranal. Chem.* **1994**, *365*, 289. (l) Mathias, M. F.; Haas, O. *J. Phys. Chem.* **1993**, *97*, 9217.

(3) Bard, A. J. *Integrated Chemical Systems*; Wiley Interscience John Wiley and Sons: New York, 1994.

(4) (a) Ashwell G. J. *Molecular Electronics*; John Wiley and Sons: New York, 1992. (b) Aviram A. *AIP Conference Proceedings 262*; American Institute of Physics: Woodbury, NY, 1992.

(5) (a) Abruna, H. D.; Denisevich, P.; Umana, M.; Meyer, T. J.; Murray, R. W. *J. Am. Chem. Soc.* **1981**, *103*, 1. (b) Denisevich, P.; Willman, K. W.; Murray, R. W. *J. Am. Chem. Soc.* **1981**, *103*, 4127. (c) Willman, K. W.; Murray, R. W. *J. Electroanal. Chem.* **1982**, *133*, 211. (d) Pickup, P. G.; Kutner, W.; Leidner, C. R.; Murray, R. W. *J. Am. Chem. Soc.* **1984**, *106*, 1991. (e) Gray, K. H.; Gould, S.; Leasure, R. M.; Musselman, I. H.; Lee, J. J.; Meyer, T. J.; Linton, R. W. *J. Vac. Sci. Technol. A* **1992**, *10*, 2679. (f) O'Toole, T. R.; Sullivan, B. P.; Meyer, T. J. *J. Am. Chem. Soc.* **1989**, *111*, 5699. (g) Gould, S.; O'Toole, T. R.; Meyer, T. J. *J. Am. Chem. Soc.* **1990**, *112*, 9490. (h) Surridge, N. A.; McClanahan, S. F.; Hupp, J. T.; Danielson, E.; Gould, S.; Meyer, T. J. *J. Phys. Chem.* **1989**, *93*, 294. (i) Surridge, N. A.; Hupp, J. T.; McClanahan, S. F.; Gould, S.; Meyer, T. J. *J. Phys. Chem.* **1989**, *93*, 304. (j) Westmoreland, T. D.; Calvert, J. M.; Murray, R. W.; Meyer, T. J. *J. Chem. Soc., Chem. Commun.* **1983**, *2*, 65. (k) Wrighton, M. S.; Frisbie, C. D.; Gardner, T. J.; Kang, D. *Microchem. Proc. JRDC-KUL Jt. Int. Symp.* **1994**, 495. (l) Huang, J.; Wrighton, M. S. *Anal. Chem.* **1993**, *65*, 2740. (m) McCoy, C. H.; Wrighton, M. S. *Chem. Mater.* **1993**, *5*, 914. (n) Talham, D. R.; Crooks, R. M.; Cammarata, V.; Leventis, N.; Schloh, M. O.; Wrighton, M. S. *NATO ASI Ser., Ser. B* **1990**, 627. (o) Leventis, N.; Schloh, M. O.; Natan, M. J.; Hickman, J. J.; Wrighton, M. S. *Chem. Mater.* **1990**, *2*, 568. (p) Oskar, O. E.; Craston, D. H.; Bard, A. J. *J. Vac. Sci. Technol. B* **1988**, 6, 1873. (q) Bard, A. J. *Integrated Chemical Systems*; John Wiley and Sons: New York, 1994; pp 1−35.

(6) Terrill, R. H.; Hatazawa, T.; Murray R. W. *J. Phys. Chem.* **1995**, *99*, 16676.

(7) Maness, K. M.; Terrill, R. H.; Meyer, T. J.; Murray, R. W.; Wightman, R. M. *J. Am. Chem. Soc.* **1996**, *118*, 10609.

(8) (a) There are reported alkyl-linked analogs:[8b−d] (b) Haozaki, O.; Ohsaka, T.; Oyama, N. *J. Phys. Chem.* **1992**, *96*, 10492. (c) Shimomura, M.; Utsugi, K.; Horikoshi, J.; Okuyama, K.; Hatozaki, O.; Oyama, N. *Langmuir* **1991**, *7*, 760. (d) Nomura, K.; Hirayama, K. *J. Macromol. Sci.-Chem.* **1989**, *A26*, 593. (e) Hillman, A. R.; Mallen, E. F. *Electrochim. Acta* **1992**, *37*, 1887.

(9) Loss in signal was observed when the film was electrolyzed repeatedly over the 1+/0 couple, suggesting that the 0-valent form is unstable or soluble.

(10) The mixed solvent is a compromise between lowered ionic resistivity but higher solubility of the viologen polymer in CH_3CN and high ionic resistances but low solubility in THF. In pure CH_3CN/Bu_4NClO_4, the films thinned over several minutes until only *ca.* 30 nm persistently remained.

(11) (a) Aoki, K.; Morita, M.; Niwa, O.; Tabei, H. *J. Electroanal. Chem.* **1988**, *256*, 269. (b) Nishihara, H.; Dalton, F.; Murray, R. W. *Anal. Chem.* **1991**, *63*, 2955.

(12) Hatazawa, T.; Terrill, R. H.; Murray, R. W. *Anal. Chem.* **1996**, *68*, 597.

(13) Majda, M. In *Molecular Design of Electrode Surfaces;* Murray, R. W., Ed.; J. Wiley: New York, 1992; Chapter IV.

(14) $E^{\circ\prime} = -656$ and -1176 mV *vs* Ag/0.01 M Ag^+, averages of E_{PEAK} values of reduction and oxidation peaks.

(15) (a) Andrieux, C. P.; Saveant, J.-M. *J. Electroanal. Chem.* **1980**, *111*, 377. (b) Laviron, E. *J. Electroanal. Chem.* **1980**, *112*, 1. (c) Pickup, P. G.; Kutner, W.; Leidner, C. R.; Meyer, T. J.; Murray, R. W. *J. Am. Chem. Soc.* **1984**, *106*, 1991. (d) Jernigan, J. C.; Chidsey, C. E. D.; Murray, R. W. *J. Am. Chem. Soc.* **1985**, *107*, 2824.

(16) (a) Shu, C.-F.; Wrighton, M. S. *J. Phys. Chem.* **1988**, *92*, 5221. (b) Lewis, T. J.; White, H. S.; Wrighton, M. S. *J. Am. Chem. Soc.* **1984**, *106*, 6947.

(17) Bock, C. R.; Connor, J. A.; Gutierrez, A. R.; Meyer, T. J.; Whitten, D. G.; Sullivan, B. P.; Nagle, J. K. *Chem. Phys. Lett.* **1979**, *61*, 522.

(18) Two gradients in series, with diffusion coefficients $D_{1,APP}$ and $D_{2,APP}$ experience the same electron flux, so the flux $j = D_{1,APP}\,C/d_1 = D_{2,APP}C/d_2$, where $d_1 + d_2 = d$, the gap width. Eliminating d_1 and d_2 gives $j = (D_{1,APP} + D_{2,APP})C/d$.

(19) (a) Monk, P. M.; Fairweather R. D.; Ingram M. D.; Duffy, J. A. *J. Chem. Soc., Perkin. Trans. 2* **1992**, *11*, 2039. (b) Koenigstein, C.; Baer, R. *Sol. Energ. Mater. Sol. Cells* **1994**, *3*, 535. (c) Imayashi, S.; Kitamura, N.; Tazuke, S.; Tokuda, K. *J. Electroanal. Chem.* **1988**, *243*, 143.

(20) Determination of the mixed valent film composition by coulometry or spectrophotometry is in principle possible, but both approaches face substantial technical difficulties.

(21) Scher, H.; Lax, M. *Phys. Rev. B* **1973**, *7*, 4491.

(22) Electrical gradients shown in Figure 6, bottom, are calculated assuming uniform current density within the gradient film. The actual electrical gradients for steady state currents under a $\Delta E = +600$ mV forward bias may differ those shown because the simple calculation ignores the built-in *Nernstian* potential gradient as well as bulk and interfacial space-charges.

(23) Electrolyzed bipotentiostatically, opposing electrodes ±150 mV relative to $E^{\circ\prime}$.

(24) Assuming 10^{-9} mol/cm^2 and using the total IDA finger surface area.